P038

Arbitrary coupling ratio multimode interference couplers in Silicon-on-Insulator

J.D. Doménech[1], **J.S. Fandiño**[2], **B. Gargallo**[2] **and P. Muñoz**[1,2]
[1]VLC Photonics S.L., Spain - david.domenech@vlcphotonics.com
[2]Universitat Politècnica de València, Spain - pmunoz@iteam.upv.es

Abstract

In this paper we present the experimental demonstration of Multimode Interference (MMI) couplers in Silicon-on-Insulator (SOI) technology with coupling ratios 95:05, 85:15, 75:25, 65:35 and 55:45. The couplers were designed using a rib waveguide Si cross-section with SiO_2 cladding, on a regular 220 nm film and 2 μm buried oxide SOI wafer. Set of devices were fabricated in two wafers with two different etch depths. The coupling ratios obtained match, with little deviations, the design targets for a wavelength range between 1525 and 1575 nm. Excess loss is conservatively estimated to be less than 2 dB.

I. Introduction

The Multimode Interference (MMI) coupler is widely used in high index contrast technologies, such as III-V and group IV material systems based PICs, since it is in general more compact, and preserves the coupling constant over a wide wavelength range. Since its inception [1], and the early demonstrations [2], multitude of papers have studied these devices: theory and design rules for canonical MMIs [3]–[5]; design rules and demonstration widened/narrowed body MMIs for arbitrary coupling ratios at a single wavelength [6] and reconfiguration using thermal tuning [7]; tolerance analysis [8] and design optimizations for different technologies [9], to name a few. In this paper we report on the design and experimental demonstration of arbitrary coupling ratio MMIs following the design rules from [6], supported by Beam Propagation Method (BPM) commercial software optimizations [10], on a Silicon-on-Insulator (SOI) platform.

II. Experimental results

The design of all the MMIs was carried out in three steps: i) cross-section analysis and 2D reduction [10], ii) analytical approach [6] and iii) numerical BPM optimization [10]. The cross-section consist of a rib waveguide in a standard SOI wafer with SiO_2 cladding. The devices were fabricated on two different wafers, A and B, using a 248 nm CMOS fabrication line. Wafers A and B had different etch depth for the rib waveguides, 130 nm (design) and 160 nm respectively from top of the Si film.3 dies per wafer were retained for measurements. A picture of the fabricated devices is shown in Fig. 2. All the layouts included focusing grating couplers (FGC) [11] for TE polarization. The *coupling ratios* for the MMIs were derived from the spectral traces measured at outputs. The results are given in Fig. 3, where the average coupling ratios and standard deviations in the wavelength range of the measurements are shown. They show good agreement with target coupling ratios. Deviations from the mean value are approximately in the range of ± 0.02. Note the additional etch depth of

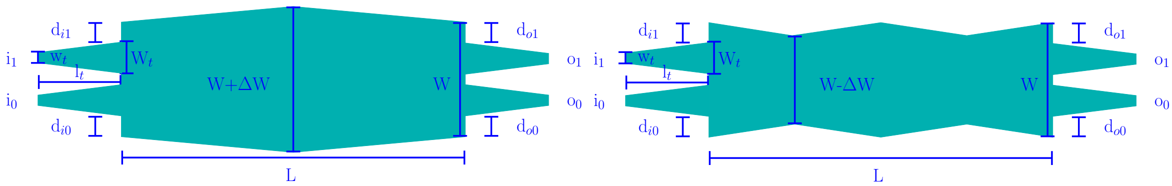

(a) (b)

Fig. 1. Multimode Interference coupler sketches, (a) Type A, B, C, D and (b) Type B Symmetrical layout. Abbreviations: L and W, MMI body length/width; d_{io} distance of input/output waveguides from the edges of the MMI; l_t input/output taper length; w_t and W_t input/output taper narrow/wide widths.

Id	#1	#2	#3	#4	#5
Ratio	95:05	85:15	75:25	65:35	55:45
Type	B Sym	B Sym	C	D	D
L	211.95	184.55	247.18	170.36	200.04
ΔW	1.44	2.53	3.26	1.5	3.34
d_{i0},d_{i1}	1.97	1.97	1.11	0.60,2.60	0.61,2.61
d_{o0},d_{o1}	1.97	1.97	1.11	2.60,0.60	2.61,0.61
W_t	2.7	2.7	2.83	2.83	2.80
Body	Double	Double	Single	Single	Single

TABLE I
MMI DESIGN PARAMETERS, LENGTHS AND WIDTHS IN μm. FOR ALL $W_t = 0.45$, L_t=50, W=10 MICRONS.

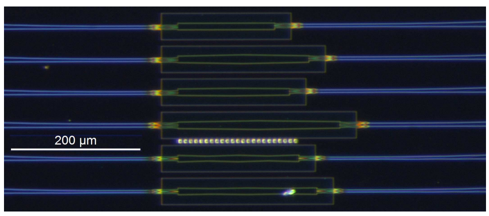

Fig. 2. Chip photograph for the fabricated MMI devices, from bottom to top MMIs #3-#7, i.e. 95:05, 85:15, 75:25, 65:35, 55:45 (non canonical) and 72:28 (canonical) splitting ratios.

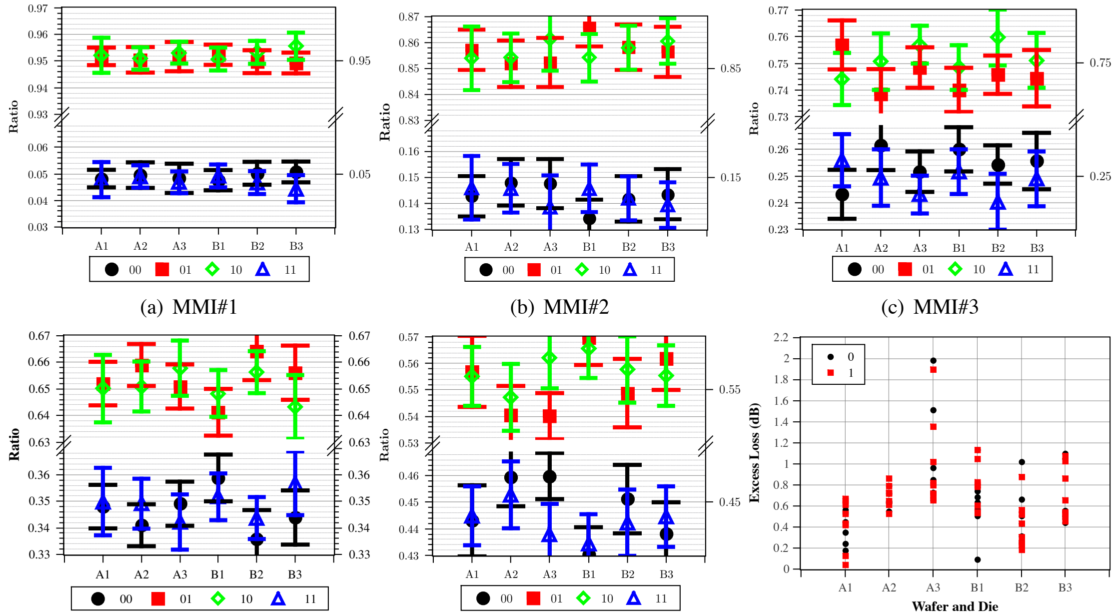

(a) MMI#1 (b) MMI#2 (c) MMI#3

(d) MMI#4 (e) MMI#5 (f) EL

Fig. 3. MMIs coupling ratio average and standard deviation, $\lambda \in [1525, 1575]$ nm, wafers A y B and dies 1, 2, 3 within each wafer.

30 nm in wafer B did not change significantly the results, as reported in [9]. The ratios are calculated from spectra obtained from adjacent different outputs, through different output FGCs. Little variations (imbalance, deviation) are observed except for a few cases, and differences in the FGCs can explain the average value deviations, e.g. MMI#5 A3 in Fig. 3-(e). An estimation for the *excess loss*, EL, is derived combining the MMI measured spectra with the spectra of reference straight waveguides. The results needed to be corrected by adding 0.4 dB, accounting for the deviations due to fiber alignments and differences in FGC performance. Consequently, an absolutely accurate value for the EL cannot be derived from these measurements. Otherwise, one should resort to full in depth statistical analysis of a larger number of samples [12] [13]. However, from these calculations, the interval on which the EL lies can be estimated at the sight of Fig. 3-(e). Inferring conservative conclusions from these graph leads to an expected EL for each MMI of less than 2 dB.

III. Conclusion

In this paper the design, fabrication and measurement of MMIs with arbitrary coupling ratio in Silicon-on-Insulator technology has been reported. The design methodology consisted on a combination of theoretical first guess and numerical optimization, using the Beam Propagation Method. The devices were fabricated in two different wafers, where the waveguides had different etch depths. Very good match between the design and experimental results was obtained in terms of the coupling ratio for the devices. All the coupling ratios were attained within the design wavelength range of 1525-1575 nm with deviations as low as ± 0.02. Minor deviations were attributed to the difference in the performance of the focusing grating couplers. Furthermore, the excess loss for the MMIs was estimated from the measurements to be less than approximately 2 dB.

The authors acknowledge the Spanish CDTI NEOTEC, MICINN TEC2010-21337, MINECO TEC2013-42332-P, FEDER UPVOV 10-3E-492, FEDER UPVOV 08-3E-008, FPI BES-2011-046100 and FPU AP2010-1595.

References

[1] R. Ulrich and G. Ankele, *Appl. Physics Lett.*, vol. 27, no. 6, 1975.
[2] E. Pennings, R. Deri *et al.*, *Appl. Physics Lett.*, vol. 59, no. 16, pp. 1926–1928, 1991.
[3] L. B. Soldano and E. C. Pennings, *J. Lightwave Technol.*, vol. 13, no. 4, pp. 615–627, 1995.
[4] M. Bachmann, P. Besse, and H. Melchior, *Appl. Optics*, vol. 33, no. 18, pp. 3905–3911, 1994.
[5] ——, *Appl. Optics*, vol. 34, no. 30, pp. 6898–6910, 1995.
[6] P.-A. Besse, E. Gini *et al.*, *J. Lightwave Technol.*, vol. 14, no. 10, pp. 2286–2293, Oct 1996.
[7] J. Leuthold and C. H. Joyner, *J. Lightwave Technol.*, vol. 19, no. 5, p. 700, May 2001.
[8] P.-A. Besse, M. Bachmann *et al.*, *J. Lightwave Technol.*, vol. 12, no. 6, pp. 1004–1009, Jun 1994.
[9] R. Halir, I. Molina-Fernandez *et al.*, *J. Lightwave Technol.*, vol. 26, no. 16, pp. 2928–2936, Aug 2008.
[10] "FieldDesigner and OptoDesigner software packages," http://www.phoenixbv.com/.
[11] F. Van Laere, T. Claes *et al.*, *IEEE Photonics Technol. Lett.*, vol. 19, no. 23, pp. 1919–1921, 2007.
[12] L. He, Y. Liu *et al. IEEE Photonics Technol. Lett.*, vol. 25, no. 14, pp. 1358–1361, 2013.
[13] W. Bogaerts, M. Fiers, and P. Dumon, *IEEE J. Selected Top. in Quantum Elect.*, vol. 20, no. 4, pp. 1–8, July 2014.